

Charge and Delocalisation Effects on the Lipophilicity of Protonable Drugs

Frédéric Reymond,^[a] Pierre-Alain Carrupt,^[b] Bernard Testa,^[b] and Hubert H. Girault*^[a]

Abstract: The transfer mechanisms of ionisable compounds of pharmaceutical interest were studied by cyclic voltammetry at the water/1,2-dichloroethane interface. The partition coefficients of the various ions were deduced from the voltammograms which were monitored as a function of aqueous pH. The dissociation constants and the partition coefficients of the neutral species were determined by a pH-metric titration technique, and the results obtained are displayed in the form of ionic partition diagrams which define the predomi-

nance domains of each species in both phases. These diagrams afford an easy interpretation of the mechanisms governing ion transfer and show how neutral species can facilitate the passage of protons from water into an organic phase and thus how ionisable compounds can modulate the pH. The change in lipophilicity between charged

and neutral forms of a given compound is discussed in terms of an intramolecular stabilisation of the charge. The nature of the substituents surrounding the charged atom as well as the degree of delocalisation of the charge are shown to contribute markedly to the stabilisation of ionic species in the organic phase. Born's solvation model is also used to illustrate qualitatively the effect of the molecular radius on the lipophilicity and to show that ions retain more water molecules when they transfer into octanol than into 1,2-dichloroethane.

Keywords: drug research • ionic partition diagrams • ITIES • lipophilicity

Introduction

Quantitative structure–activity and structure–property relationships (QSAR/QSPR) are of great importance in medicinal chemistry and biochemistry, because they can accelerate the development of new compounds for use as drugs, materials or additives by computer screening of molecular structures that can predict the desired properties prior to laboratory tests. QSAR/QSPR correlations have now been established to reflect intermolecular interactions in dense media.^[1] Because of the complexity of solvent effects,^[2] these correlations usually involve several parameters, such as the polarity and polarisability of the solvents, their abilities as a hydrogen-bond donor or acceptor, as well as dispersion and repulsion interactions.^[3] Indeed, the $\log P$ parameter is also a solvational characteristic since it is directly related to the change in the Gibbs energy of solvation of a solute between two solvents. Much attention has been paid over the past two

decades to the calculation of partition coefficients directly from the solute structure or the solvation energy in order to connect the lipophilicity to the biological activity.

On account of the lack of experimental techniques which permit the measurement of charged species, such relationships have unfortunately been limited to neutral compounds. As a consequence, membrane permeation of ions has generally been neglected, but this assumption is becoming suspect^[4,5] as a result of an increasing amount of experimental evidence which supports ion partitioning.^[6–10] Furthermore, novel experimental techniques have revealed marked variations in the partition coefficients of ionised species under biomimetic conditions with respect to changes in the chemical structures and experimental conditions.^[11] In order to increase our understanding of the intermolecular forces responsible for these variations, we have investigated the partition behaviour of a series of compounds as a function of their ionisation state to obtain their pH-lipophilicity profiles. Electrochemical measurement at the interface between two immiscible electrolyte solutions (ITIES) has already proved to be a technique suitable for the measurement of the $\log P$ of ionic species, and it is used here to determine the various mechanisms which govern drug transfer and to explain the different affinity of charged and neutral forms of a compound towards an organic phase. The present work shows how molecular volume, intramolecular distance between charges and intramolecular charge delocalisation (i. e. the distribution of the electronic charge in a molecule over more than just one

[a] Prof. H. H. Girault, F. Reymond
Laboratoire d'Electrochimie, Ecole Polytechnique Fédérale de Lausanne
CH-1015 Lausanne (Switzerland)
Fax: (+41) 21-693.36.67
E-mail: hubert.girault@epfl.ch

[b] P.-A. Carrupt, B. Testa
Institut de Chimie Thérapeutique, Section de Pharmacie, Université de Lausanne
CH-1015 Lausanne (Switzerland)

atom) affect solvation, and, as such, is the first step towards the incorporation of ion properties into QSPR studies. This is of great significance in pharmacokinetics and correlations which incorporate charged species, and it should also lead to an improvement of QSAR predictions.

Theoretical Background

Transfer at the ITIES: At a liquid/liquid interface, both the neutral (N) and the ionic (I) form of a compound may, a priori, be present in both phases. At the equilibrium, the distribution of a charged species between the organic and the aqueous phase is dependent upon the potential and is expressed by the Nernst equation for the ITIES [Eq. (1)]:^[12] where a_I and c_I are the activity and the concentration of I in water (w) and in the organic

$$\Delta_o^w \phi = \Delta_o^w \phi_I^0 + \frac{RT}{z_I F} \ln \left(\frac{a_I^o}{a_I^w} \right) = \Delta_o^w \phi_I^{0'} + \frac{RT}{z_I F} \ln \left(\frac{c_I^o}{c_I^w} \right) \quad (1)$$

phase (o), respectively; z_I is the charge of I, $\Delta_o^w \phi$ represents the Galvani potential difference across the interface, $\Delta_o^w \phi_I^0$ is the standard ion transfer potential and $\Delta_o^w \phi_I^{0'}$ the formal ion transfer potential of I. The standard ion transfer potential is, in fact, the standard Gibbs energy of transfer ($\Delta G_{tr,I}^{0,w \rightarrow o}$) expressed on a potential scale, since these two quantities are related by Equation (2), where μ_I^0 is the standard chemical potential.

$$\Delta_o^w \phi_I^0 = \frac{\Delta G_{tr,I}^{0,w \rightarrow o}}{z_I F} = \frac{(\mu_I^{0,o} - \mu_I^{0,w})}{z_I F} \quad (2)$$

Abstract in French: *Les mécanismes de transfert de composés ionisables d'intérêt pharmaceutique ont été étudiés par voltamétrie cyclique à l'interface eau/1,2-dichloroéthane. Les coefficients de partage de ces ions ont été déduits des voltammogrammes enregistrés à différents pH de la phase aqueuse. Les constantes de dissociation et les coefficients de partage des espèces neutres ont été déterminés par une technique pH-métrique de titrage et les résultats obtenus sont représentés sous la forme de diagrammes de partage ionique qui définissent les domaines de prédominance de chaque espèce présente dans les deux phases. Ces diagrammes permettent d'interpréter facilement les mécanismes gouvernant le transfert d'ions et ils montrent comment les espèces neutres peuvent faciliter le transfert de protons de l'eau à la phase organique. Les études menées ici montrent ainsi comment des composés ionisables peuvent moduler le pH d'un milieu. D'autre part, les changements de lipophilie entre les formes neutre et chargée(s) d'un composé donné sont discutés en termes de stabilisation intramoléculaire de la charge. Il a été mis en évidence que la nature des substituants entourant l'atome chargé de même que le degré de délocalisation de la charge contribuent profondément à la stabilisation des espèces ioniques en phase organique. Le modèle de solvation de Born est aussi employé pour illustrer qualitativement l'effet du rayon moléculaire sur la lipophilie et pour montrer que les ions retiennent plus de molécules d'eau lorsqu'ils transfèrent dans l'octanol que dans le 1,2-dichloroéthane.*

In cyclic voltammetry, the difference in the electrical potential across the interface is swept linearly between two limiting values, which modifies all the thermodynamic equilibria in the vicinity of the interface. As expressed by Equation (1), the distribution of the various species in the two adjacent phases changes during a potential sweep which induces the transfer of an ion I across the interface when the potential approaches its standard transfer potential $\Delta_o^w \phi_I^0$. This flux of charges across the interface leads to a measurable current which is recorded as a function of the applied potential (such curves are called voltammograms and typical examples are shown in Figure 3). Upon transfer of a species, a concentration gradient is thus established along which the ions may diffuse on both sides of the interface. On the very short experimental time scale, the bulk of each phase remains unchanged, and the dissociation equilibria are maintained during a potential sweep.

For kinetically fast (i.e. electrochemically reversible) ion transfer where the passage across the interface is limited by the diffusion at the interface, Equation (1) is valid at any rate of the potential sweep. When the standard transfer potential of an ion is approached, the current rises because the flux of ions across the interface increases. If higher potentials are applied, then the interfacial concentration begins to drop because the diffusion is no longer fast enough to supply the amount of ions required to compensate for the displacement of the equilibrium given by the Nernst equation. As a result, the current falls yielding the characteristic peak shape of cyclic voltammograms.

Moreover, the ratio a_I^o/a_I^w is, by definition, the partition coefficient of the ionic species I between the two phases, P_I , which is generally given on a logarithmic scale. When dilute solutions and equal volumes of the two adjacent phases are used (as in the present study), the activities can be replaced by the concentrations to evaluate $\log P_I$, since the logarithm of the ratio of the activity coefficients can then be neglected. The partition coefficient of an ion is dependent on the potential^[13] and is directly deduced from Equation (1). In terms of concentration, we obtain Equation (3),

$$\log P_I = \frac{z_I F}{RT \ln 10} (\Delta_o^w \phi - \Delta_o^w \phi_I^{0'}) = \frac{z_I F}{RT \ln 10} \Delta_o^w \phi - \frac{\Delta G_{tr,I}^{0,w \rightarrow o}}{RT \ln 10} = \log P_I^{0'} + \frac{z_I F}{RT \ln 10} \Delta_o^w \phi \quad (3)$$

where $\log P_I^{0'}$ is the formal partition coefficient of I, which represents the proportion of ions present in each phase if the interface is not polarised.

In contrast to ions, the distribution of the neutral form of a compound between the two phases does not depend on the potential and pH. It is thus a constant which is directly connected to its formal Gibbs energy of transfer [Eq. (4)].

$$\log P_N = \log \left(\frac{c_N^o}{c_N^w} \right) = - \frac{\Delta G_{tr,N}^{0,w \rightarrow o}}{RT \ln 10} \quad (4)$$

Finally, following the definition of dissociation constants, it is easy to show that acid/base equilibria in water and in the organic phase (K_a^w and K_a^o , respectively) can be expressed by the partition coefficients of all the species involved in the equilibrium. In the case of a dibase (where I^{2+} stands for the doubly protonated species and I^+ for the singly protonated form of the neutral base N), the first and second dissociation constants in the organic phase can be directly assessed by Equations (5) and (6).

$$pK_{a1}^o = pK_{a1}^w - \log \left(\frac{P_{I^+}^{0'} P_{H^+}^{0'}}{P_{I^{2+}}^{0'}} \right) \quad (5)$$

$$pK_{a2}^o = pK_{a2}^w - \log \left(\frac{P_N P_{H^+}^{0'}}{P_{I^+}^{0'}} \right) \quad (6)$$

Consequently, $\Delta_o^w \phi_I^0$, $\Delta G_{tr,I}^{0,w \rightarrow o}$, $\log P_I^{0'}$ and pK_a^o can all be deduced from cyclic voltammetry experiments at the ITIES, and it will be shown below how the evolution of the voltammograms with aqueous pH reflects the transfer mechanisms of the various species present in the electrochemical cell as well as the lipophilicity of ions.

Effect of the molecular radius on ion partitioning: Following Born's solvation model, the Gibbs energy of ion-solvent interaction, ΔG_{IS}^o , can be

estimated by the difference between the charging work of a sphere in an electric medium α and the discharging work of this sphere in vacuum. $\Delta G_{\text{IS}}^{\alpha}$ represents the difference in the chemical potential between one mole of ions and one mole of neutral molecules of equal size, and it is expressed as Equation (7)^[14], where e is the charge of the proton, N_{A} is Avogadro number, r is the molecular radius, ϵ_0 is the vacuum permittivity and ϵ_r^{α} the dielectric constant of the phase α .

$$\Delta G_{\text{IS}}^{\alpha} = -\frac{z^2 e^2 N_{\text{A}}}{8\pi\epsilon_0 r} \left(1 - \frac{1}{\epsilon_r^{\alpha}}\right) \quad (7)$$

As the dielectric constant of solvents varies between 2 and 80, $\Delta G_{\text{IS}}^{\alpha}$ is always negative and the solvent definitely stabilises the ion. This stabilisation is much larger for water than for octanol or 1,2-dichloroethane, since their dielectric constants are 78 and ≈ 10 , respectively (ϵ_r^{α} is approximately the same for octanol and 1,2-dichloroethane). As the partition coefficients represent the difference in solvation energy between two solvents, the $\log P$ difference between a charged and a neutral species $\text{diff}(\log P_{\text{I-N}}^0)$ can be approximated by means of Equation (7) which yields Equation (8).

$$\text{diff}(\log P_{\text{I-N}}^0) = \frac{-(\Delta G_{\text{IS}}^{\text{o}} - \Delta G_{\text{IS}}^{\text{w}})}{RT \ln 10} = \frac{z^2 e^2 N_{\text{A}}}{8\pi\epsilon_0 r} \frac{\epsilon_r^{\text{o}} - \epsilon_r^{\text{w}}}{\epsilon_r^{\text{o}} \epsilon_r^{\text{w}}} \quad (8)$$

$$\text{where: } \text{diff}(\log P_{\text{I-N}}^0) = \log P_{\text{I}}^0 - \log P_{\text{N}}^0 \quad (9)$$

Since $\epsilon_r^{\text{w}} > \epsilon_r^{\text{o}}$, $\text{diff}(\log P_{\text{I-N}}^0)$ is always negative, this confirms that the stabilisation of the charged species is better in water than in organic solvents. As shown in Figure 1 for singly and doubly charged ions, this effect is larger for ions with a smaller molecular radius.

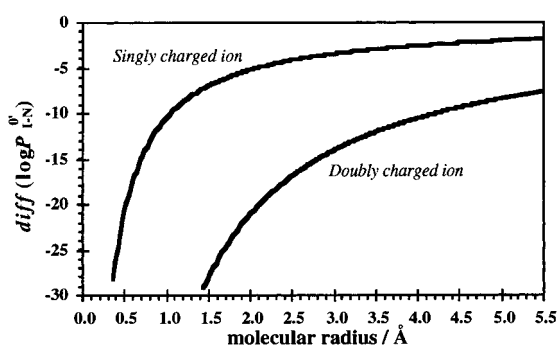


Figure 1. The difference in the partition coefficients between the ionic and the neutral forms of a compound as a function of its molecular radius. The calculation is based on Born's solvation model, and the evolution of $\text{diff}(\log P_{\text{I-N}}^0)$ is shown for singly and doubly charged ions.

Born's theory neglects the dielectric saturation and assumes that the dielectric constant around the ion ϵ_r^{α} is equal to that in the bulk ϵ_r^{α} . An improved prediction of the Gibbs energy of solvation can be obtained by the use, for instance, of the Abraham and Liszi model,^[15] where $\Delta G_{\text{IS}}^{\alpha}$ is divided into an electrostatic and a neutral contribution. However, with regard to the $\text{diff}(\log P_{\text{I-N}}^0)$ values, the correction for the dielectric saturation becomes negligible so that both models provide the same results. Equation (8) can therefore be used to estimate $\text{diff}(\log P_{\text{I-N}}^0)$ without generating much larger errors than the more sophisticated models, and it will be shown below that Born's theory already allows the qualitative explanation of the difference in the partition coefficients of the charged and the neutral species.

Experimental Section

Amfepramone (AMF; extracted and purified from tablets), *N,N*-diethylaniline (DEAN), 3,5, *N,N*-tetramethylaniline (TMAN), *N*-methylephe-

drine (ME)(all from Fluka) and quinine (Q)(Sigma) were of the highest purity available. The organic solvent was analytical grade 1,2-dichloroethane (Merck) and was used without further purification. All necessary precautions were taken in the handling of 1,2-dichloroethane to avoid inhalation and skin contact.^[16] Deionised water (Milli-QSP reagent water system, Millipore) was employed throughout and bis(triphenylphosphoranyliden)ammonium tetrakis(4-chlorophenyl)borate (BTTPATPBCl) was used as the supporting organic electrolyte. It was prepared by metathesis of bis(triphenylphosphoranyliden)ammonium chloride (BTTPACl) (Fluka) and potassium tetrakis(4-chlorophenyl)borate (KTPBCl) (Lancaster) and recrystallised twice from methanol.

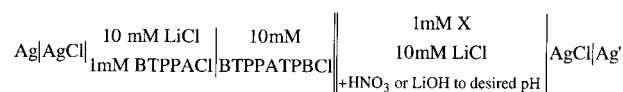
Cyclic voltammetric studies were conducted using a home-made four-electrode potentiostat with *iR* drop compensation of a design similar to that given in ref. [13]. The difference in applied potentials, E , is defined as the potential applied between the two reference electrodes, and it is related to the Galvani potential difference across the interface by Equation (10),

$$E = \Delta_{\text{o}}^{\text{w}} \phi + \Delta E_{\text{ref}} \quad (10)$$

where ΔE_{ref} depends strongly on the nature of the two reference electrodes, so that E refers only to the electrochemical cell used and represents a totally arbitrary scale. Thus, the half-wave potentials, $E_{\text{I}}^{1/2}$, deduced from the voltammograms were all referenced against tetramethylammonium (TMA⁺), because its formal transfer potential in the absolute Galvani potential scale has already been established ($\Delta_{\text{o}}^{\text{w}} \phi_{\text{TMA}^+}^0 = 160 \text{ mV}^{[17]}$). In this manner, the values of $E_{\text{I}}^{1/2}$ were further transposed to the absolute scale by applying Equation (11).

$$E_{\text{I}}^{1/2} - \Delta_{\text{o}}^{\text{w}} \phi_{\text{I}}^0 = E_{\text{TMA}^+}^{1/2} - \Delta_{\text{o}}^{\text{w}} \phi_{\text{TMA}^+}^0 \quad (11)$$

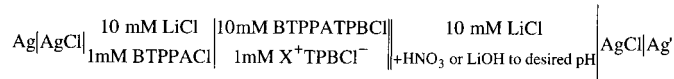
All the molecules under study were first dissolved in the aqueous phase, the pH of which was set to the desired value by the addition of HNO₃ or LiOH (Fluka). The volumes of the aqueous and organic phases were always equal (1.7 mL), and all the experiments were performed in Cell 1 (Scheme 1), where X stands for each compound mentioned at the beginning of this section.



Scheme 1. Cell 1.

In such a cell, the potential window was limited by the transfer of Cl⁻ and Li⁺ at low ($\Delta_{\text{o}}^{\text{w}} \phi_{\text{Cl}^-}^0 = -470 \text{ mV}^{[18]}$) and high potentials ($\Delta_{\text{o}}^{\text{w}} \phi_{\text{Li}^+}^0 = 576 \text{ mV}^{[19]}$). In this manner, the experimental domain could not be expanded beyond these two potential values, and it is delimited by lines *a* and *b* in the ionic partition diagrams. In this paper, the transfer of a cation from water to 1,2-dichloroethane is defined as a positive current. This relates to the fact that the potential of water is made more positive with respect to that of the organic phase on the forward scan, a convention valid for all ITIES experiments. It should also be stressed that the current peaks obtained by cyclic voltammetry correspond to a flux of ions across the water/1,2-dichloroethane interface and are in no way redox in nature.

For several compounds, the cyclic voltammetry experiments were repeated using Cell 2 (Scheme 2) (X⁺ represents protonated *N,N*-diethylaniline,



Scheme 2. Cell 2.

3,5, *N,N*-tetramethylaniline or *N*-methylephedrine), where their ionic form was dissolved in the organic phase after formation of a salt soluble in 1,2-dichloroethane and following the same procedure as for the supporting electrolyte BTTPATPBCl.

Finally, the partition coefficients of the neutral species and all the $\text{pK}_{\text{a}}^{\text{w}}$ values were measured by pH-metric two-phase titration (SiriusPCA101, Sirius Anal. Instruments, UK).

Results and Discussion

Monobases: A series of monobases (Figure 2) was studied by cyclic voltammetry to determine their Gibbs energy of transfer and their lipophilicity profile. These compounds were selected on the basis of their significance in pharmacology and chemistry. All these compounds possess one protonation/deprotonation site; they are ionised below their pK_{a1}^w and are neutral above it; thus they modify their transfer behaviour according to the aqueous pH. This is illustrated in Figure 3, which shows the evolution of the voltammograms obtained for *N*-methylephedrine at four different aqueous pH values. Below pK_{a1}^w , the half-wave potential remains constant, within experimental error, and the current decreases as the pH approaches pK_{a1}^w as a result of the decrease in the concentration of protonated *N*-methylephedrine. Above pK_{a1}^w , the half-wave potential shifts by RT/zF mV per pH unit, and the current peak is a result of the transfer of a proton facilitated by the neutral *N*-methylephedrine present in the organic phase which behaves as an ionophore for the proton. Here also, the maximum forward peak current diminishes with increasing pH because it is limited by the proton concentration.

All the results obtained by cyclic voltammetry are given in Table 1, along with the values of the Gibbs energy of transfer, of the dissociation constants and of the partition coefficients. This data is used to draw the ionic partition diagram of each

Table 1. Physicochemical parameters of the determination of the water/1,2-dichloroethane partition behaviour of the series of monobases shown in Figure 2.

	<i>N</i> -Methylephedrine	Amfepramone	<i>N,N</i> -Diethylaniline	3,5, <i>N,N</i> -Tetramethylaniline
$\log P_N$	1.61 ± 0.09	3.65 ± 0.09	4.22 ± 0.04	4.01 ± 0.03
pK_{a1}^w	9.00 ± 0.01	8.80 ± 0.01	6.80 ± 0.02	5.52 ± 0.01
$\Delta_s^w \phi_i^{(a)}$	163 ± 6	36 ± 7	135 ± 14	170 ± 12
$\log P_i^{(b)}$	-2.76 ± 0.10	-0.61 ± 0.12	-2.28 ± 0.23	-2.87 ± 0.20
$pK_{a1}^{(c)}$	14.43 ± 0.22	13.95 ± 0.23	9.71 ± 0.29	8.05 ± 0.26
$\text{diff}(\log P_{I-N}^w)$	-4.37 ± 0.14	-4.26 ± 0.15	-6.50 ± 0.23	-6.88 ± 0.20

[a] Given in mV. [b] Calculated by Equation (3). [c] Calculated with a value of 549 ± 10 mV for $\Delta_s^w \phi_{H^+}^{(21)}$ and by Equation (6).

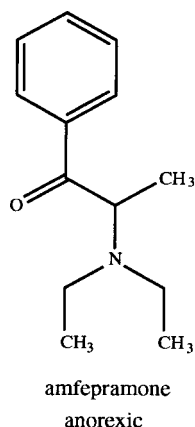
compound investigated by following the methodology described in a previous study.^[20]

N-Methylephedrine (ME) and amfepramone (AMF) were chosen for the similarity of their chemical structures. Both compounds have the same transfer behaviour, and the mean values of the formal transfer potential deduced from the voltammograms obtained with Cells 1 and 2 are used to draw their ionic partition diagrams (Figure 4). The experimental results are also given in order to show the good reproducibility of the measurements.

As expected from the principle of ionic partition diagrams, the interfacial potential required to transfer the ionised form

of both *N*-methylephedrine and amfepramone from water to 1,2-dichloroethane is constant at a pH below their respective pK_a^w , and the horizontal segments in Figure 4 correspond to their values of formal transfer potential. Above their pK_a^w however, a proton is transferred from water to 1,2-dichloroethane upon positive polarisation of the interface, so that neutral ME and AMF present at the organic side of the interface become protonated. These results show that the neutral form of acids and bases may reduce the Gibbs energy of transfer of the proton as a result of interfacial protonation and deprotonation reactions, respectively. Such a mechanism is of great importance in pharmacology, because the proton concentration is very tightly regulated in functional biological systems. Numerous pathologies are linked to the dysfunction of pH regulation, but recent studies have shown that com-

A) Monobases:



B) Dibases:

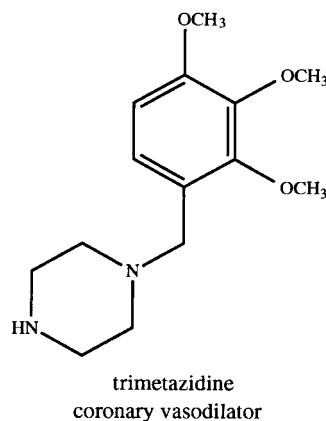
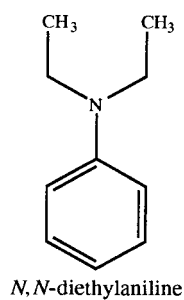
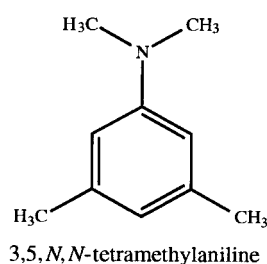
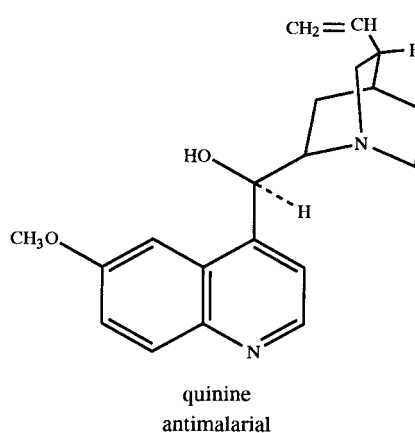
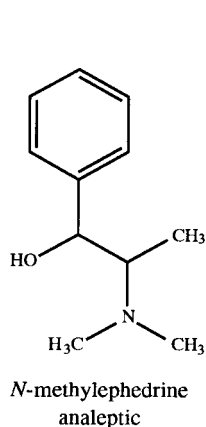


Figure 2. Chemical structures of the compounds investigated.

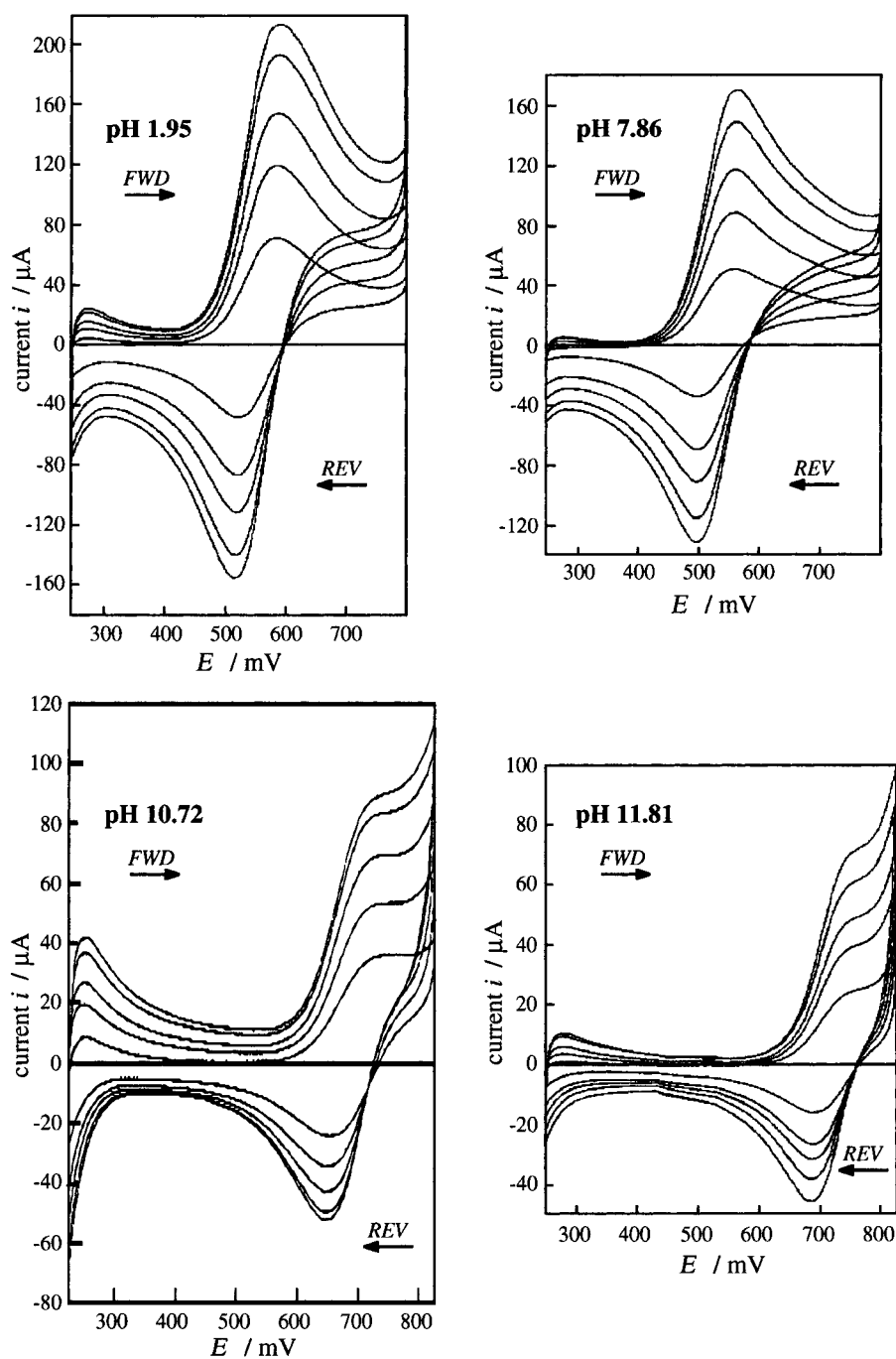


Figure 3. Typical cyclic voltammograms obtained for the transfer of a monobase across the water/1,2-dichloroethane interface. The dependence of the current waves on the aqueous pH is shown here for *N*-methylephedrine at five scan rates (10, 30, 50, 80 and 100 mV s^{-1}). The recorded current is positive on the forward scan (FWD) which signifies that positive ions transfer from water into 1,2-dichloroethane. On the reverse scan (REV), these ions transfer back into water thus generating a negative current.

pounds such as nigericin,^[22] azapropazone,^[23] piroxicam,^[24] chloroquine^[25] or tenidap^[26, 27] are able to correct for these dysfunctions. The representation of the data as an ionic partition diagram allows us to understand how ionisable compounds can facilitate the transfer of protons from an aqueous phase to another medium (such as a cellular membrane) and affords a useful way to interpret the behaviour of pH-modulating agents in biological environments.

The formal transfer potentials of *N*-methylephedrine and amfepramone differ by 127 mV, which indicates that AMFH⁺ is significantly more lipophilic than MEH⁺. Evidently, this also applies to the neutral form of these compounds, and the difference between the partition coefficients of these two species is approximately the same: $\log P_{\text{AMF}} - \log P_{\text{ME}} = 2.04$ and $\log P_{\text{AMFH}^+}^0 - \log P_{\text{MEH}^+}^0 = 2.15$. This result is not surprising, because the delocalisation of the charge is very similar for both AMFH⁺ and MEH⁺. As a consequence, the affinity of both AMFH⁺ and MEH⁺ for the organic phase remains relatively high after protonation, and this is illustrated by their $\text{diff}(\log P_{\text{I-N}}^0)$ values (-4.37 for ME and -4.26 for AMF), which are smaller than the value of -5 generally found in water/1,2-dichloroethane. This is in good agreement with Born's solvation model which shows that ions with a delocalised charge behave as larger ions than those possessing a localised charge. This is a consequence of the fact that the attractive forces between the charge and each solvating water molecule are weaker with a delocalised charge, which results in a smaller hydrophilicity and thus in a smaller change in the value of $\log P$ between neutral and protonated species.

It is of interest to note that the experimental values obtained for $\text{diff}(\log P_{\text{I-N}}^0)$ are generally ≈ -3 for octanol/water. With respect to Figure 1, this indicates that the molecular radius is $\approx 1.2 \text{ \AA}$ larger in octanol than in 1,2-dichloroethane.

Consequently, the ions are likely to retain more water molecules when they transfer into octanol, which can be explained by the larger solubility of water in octanol than in 1,2-dichloroethane and by the H-bonding capacity of octanol which is almost as large as that of water.

Otherwise, the absolute values of the partition coefficients for both the neutral and the protonated species are quite different (AMF and ME are separated by approximately two $\log P$ units). This originates from the replacement of the

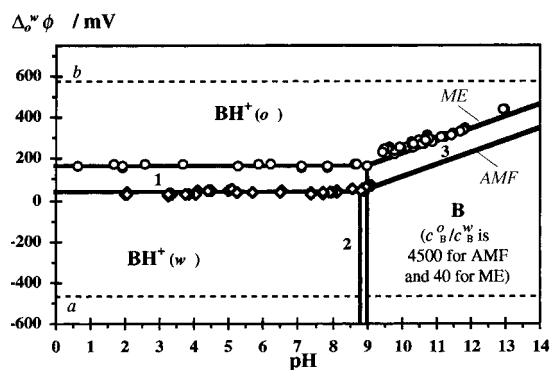


Figure 4. Ionic partition diagram of *N*-methylephedrine (ME) and amfepramone (AMF) in water/1,2-dichloroethane at 25 °C. The experimental values \circ were deduced from the voltammograms and transposed to the TATB scale, while the boundary lines (bold) were determined from the mean value of $\Delta_0^w \phi_{\text{BH}^+}^o$. Lines *a* and *b* delimit the experimental domain for Cells 1 and 2. As $\log P_B$ is positive, the neutral form of these bases was situated largely in the organic phase.

hydroxyl group in ME by a carbonyl group in AMF, which has no H-bond donating capacity. Moreover, it has been noted from our solvatochromic analysis of 1,2-dichloroethane/water,^[28] that the lengthening of an alkyl chain causes an increase of $\approx 0.5 \log P$ unit per methylene group, which is equal to the CH_2 -fragmental constant that can be deduced from the values of the Gibbs energies of transfer for the tetraalkyl ammonium series.^[12, 29] These two factors act in the same direction in the present case and constitute the main contributions to the greater lipophilicity of amfepramone.

With substituted anilines, similar considerations can be deduced from their respective ionic partition diagrams (Figure 5). 3,5,*N,N*-Tetramethylaniline (TMAN) contains four methyl groups, whereas two ethyl groups are attached to the nitrogen atom in *N,N*-diethylaniline (DEAN). Thus, it is not surprising to find very close $\log P$ values for these two compounds.

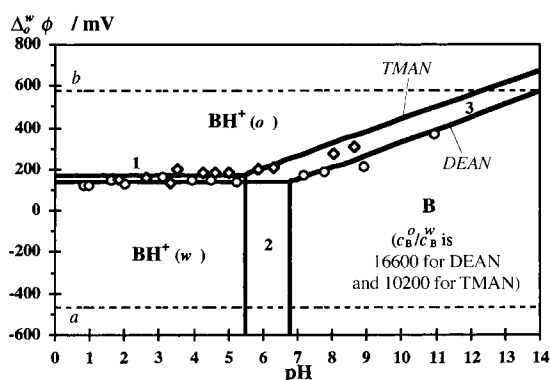


Figure 5. Ionic partition diagram of *N,N*-diethylaniline (DEAN) and 3,5,*N,N*-tetramethylaniline (TMAN) in water/1,2-dichloroethane at 25 °C.

The difference in the lipophilicity of the two charged species is markedly larger than for the neutral species: $\log P_{\text{DEANH}^+}^o - \log P_{\text{TMANH}^+}^o = 0.59$. This is due to the fact that the two methyl groups on the phenyl substituent of TMANH⁺ cannot mask the charge on the nitrogen atom. As the delocalisation is more efficient with ethyl than with methyl

substituents, it is logical that TMANH⁺ is more hydrophilic than DEANH⁺, but to a smaller degree than that expected from the CH_2 -fragmental constant.

Interestingly, the $\text{diff}(\log P_{\text{I-N}}^o)$ values are much larger in this example than in the case of AMF and ME, since they are found to be -6.88 for TMANH⁺ and -6.50 for DEANH⁺. This suggests that the solvation of these cations is very strong in water; thus, it is quite difficult to remove the aqueous solvation shell during their transfer into the organic phase. Indeed, in spite of the presence of an aryl group, the charge on the nitrogen atom cannot delocalise as well as in MEH⁺ and AMFH⁺, because aromaticity must be maintained in the phenyl substituent and because no lone pair of electrons can partially mask the charge. Compared to the above example, only two substituents can favour delocalisation in TMANH⁺ and DEANH⁺. This discrepancy results in a smaller mean molecular radius for the substituted anilines and, in addition to the respective molecular weight of these four compounds, explains the very high $\text{diff}(\log P_{\text{I-N}}^o)$ values of TMANH⁺ and DEANH⁺. With respect to Born's model, this result suggests that these ions have a smaller molecular radius, since their charge is localised. It should also be pointed out that TMANH⁺ and DEANH⁺ have approximately the same formal Gibbs energy of transfer as TMA⁺ ($\Delta G_{\text{tr, TMA}^+}^{o, w \rightarrow o} = 15.4 \text{ kJ mol}^{-1}$). As they are larger in size, this implies that they are even more hydrophilic than TMA⁺ and that their charge is very exposed to ion-dipole interactions.

Dibases: The transfer behaviour of quinine (Figure 2) was investigated by cyclic voltammetry at the water/1,2-dichloroethane interface. All the data needed to draw the ionic partition diagrams of quinine (HQ), as well as the values of the partition coefficients of each form of this compound, were deduced from the voltammograms and are presented in Table 2. Quinine is an antimalarial drug which is especially valuable for the treatment of severe illness caused by multi-drug-resistant strains of *Plasmodium falciparum* parasites.^[31] Because quinine is a base, high concentrations can build up in the acidic food vacuoles of *P. falciparum*,^[32, 33] whose primary function is the proteolysis of ingested red-cell haemoglobin in order to provide the parasite with essential amino acids. It has been suggested that HQ may act by raising the intravacuolar

Table 2. Physicochemical parameters for the determination of the partitioning of quinine and trimetazidine at the water/1,2-dichloroethane interface.

	Quinine	Trimetazidine ^[30]
$\log P_N$	2.41 ± 0.08	1.04 ± 0.06
$\Delta_0^w \phi_{\text{I}^+}^o / \text{mV}$	157 ± 19	291 ± 9
$\log P_{\text{I}^+}^o$	-5.31 ± 0.64	-9.84 ± 0.30
$\text{diff}(\log P_{\text{I-N}}^o)$	-7.72 ± 0.65	-10.88 ± 0.31
$\text{p}K_{\text{a1}}^w$	4.48 ± 0.02	4.54 ± 0.02
$\text{p}K_{\text{a1}}^o$ [a]	10.02 ± 0.70 [b]	6.85 ± 0.38 [b]
$\Delta_0^w \phi_{\text{I}^+}^o / \text{mV}$	85 ± 14	162 ± 9
$\log P_{\text{I}^+}^o$	-1.44 ± 0.24	-2.74 ± 0.15
$\text{diff}(\log P_{\text{I-N}}^o)$	-3.85 ± 0.25	-3.78 ± 0.16
$\text{p}K_{\text{a2}}^w$	8.51 ± 0.01	9.14 ± 0.02
$\text{p}K_{\text{a2}}^o$ [c]	14.07 ± 0.30 [b]	14.77 ± 0.24 [b]

[a] Calculated with Equation (5). [b] Calculated with $\Delta_0^w \phi_{\text{H}^+}^o = 549 \pm 10 \text{ mV}$.^[21] [c] Calculated with Equation (6).

pH,^[34, 35] by interfering with parasite DNA/RNA biosynthesis^[36] or by inhibiting enzymes through direct drug binding.^[37, 38] It has also recently been proposed^[39] that quinine inhibits heme polymerase in parasitic food vacuoles, thereby disrupting heme conversion into an insoluble crystalline material called hemozoin or malaria pigment. Heme is a by-product of haemoglobin degradation and it is highly toxic for malaria plasmodes.^[57] In this manner, the degradation of haemoglobin is rapidly blocked, which then halts the growth of the parasites.

Quinine has the same structure as quinidine except for the configuration at the secondary alcohol group (see Figure 2); however, the measured formal transfer potential of the mono- and diprotonated forms of quinine and quinidine are not absolutely equal, which implies that the epimeric relation of these two compounds is reflected in a slight difference in their lipophilicity ($\Delta_{\phi}^w \phi_{\text{HOH}_2^{2+}}^0 = 157$ mV (quinine) and 162 mV (quinidine)^[20] while $\Delta_{\phi}^w \phi_{\text{HOH}^+}^0 = 85$ and 80 mV, respectively). Despite its alcohol function, no current wave could be attributed to the transfer of the negatively charged form of quinine, which explains why we have treated it as a dibase instead of an ampholyte to draw up its ionic partition diagram (Figure 6).

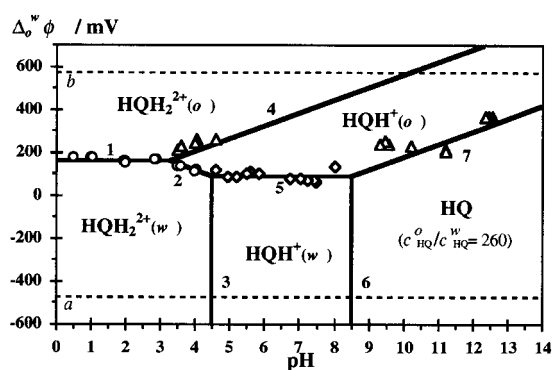


Figure 6. Ionic partition diagram of quinine in water/1,2-dichloroethane at 25°C.

Quinine is the largest molecule studied here, but it does not have the highest lipophilicity (c.f. Tables 1 and 2). The very important water affinity of the hydroxyl group of quinine is totally compensated by the quinoline function, which is very

stable in organic solvents (for comparison, reported values of the lipophilic fragmental constant of alkyl-OH is -1.45 in octanol, whereas $\log P_{\text{quinoline}}$ is 2.03 ^[40]). If protonated quinolinium remains aromatic, then the positive charge can easily delocalise, and $\text{diff}(\log P_{\text{HOH}^+}^0)$ is -3.88 , which is slightly less negative than the common value of -5 discussed above. This suggests that aromaticity in the quinolinium group significantly favours the solvation of HQH^+ in the organic phase.

For the doubly charged species, the position of boundary line 1 is located at moderately positive potentials. Thus, HQH_2^{2+} requires only a relatively small energy to transfer from water into 1,2-dichloroethane; thus, its transport across biological membranes should be relatively easy.

With doubly charged ions, it has been deduced from, as yet unpublished, results^[52] that $\text{diff}(\log P_{\text{L}^+-\text{N}}^0)$ is about -11 ; thus, the molecular radius should be about 3.8 Å, as can be deduced from Figure 1. This is in good agreement with the stronger interactions induced by the introduction of a second charge and with the number of solvent molecules needed to form the first solvation shell, which is larger in doubly than in singly charged ions. However, if the two charges are far apart then the ion should not be considered as one dication but rather as two monocations, because the solvent molecules are not attracted in the same way by two single charges as they are by one double charge.

In this manner, Born's solvation model tends to show that HQH_2^{2+} may not be considered as a dication, but as two monocations. Indeed, if $\text{diff}(\log P_{\text{HOH}^+}^0)$ is approximately the same as for the above monobases, $\text{diff}(\log P_{\text{HOH}_2^{2+}}^0)$ is only -7.72 , which is much less than the approximated value of ≈ -11 found, for instance, for trimetazidine^[30] (see Figure 2, and the corresponding experimental data in Table 2). For these two species, the electrostatic potential, obtained by AM1 semiempirical calculation (Spartan 5.0, Wavefunction Inc., Irvine USA) is displayed in Figure 7 in order to localise the charge.

From Figure 7 it can be clearly seen that doubly charged trimetazidine TMZH_2^{2+} possesses a very positive charge density around the two protonated nitrogen atoms, while two well-defined sites of less positive potential appear in HQH_2^{2+} . In HQH_2^{2+} , the two charges are sufficiently distant to behave as separate single charges with respect to the

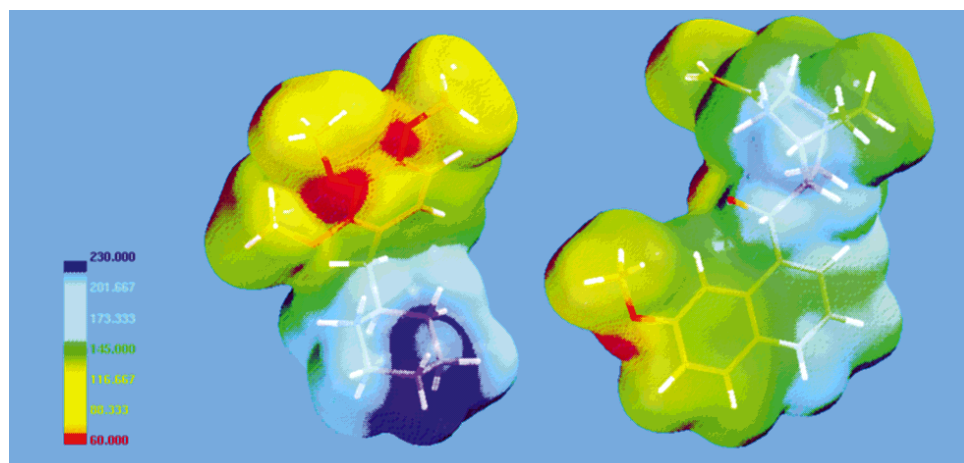


Figure 7. AM1 semiempirical calculation of the electrostatic potential surrounding doubly charged forms of trimetazidine (left) and quinine (right), respectively. The electrostatic potential increases linearly from red to dark blue.

surrounding water molecules, and, in terms of lipophilicity, the value of $\text{diff}(\log P_{\text{HOH}_2^+ - \text{HO}}^0)$ is almost twice that of $\text{diff}(\log P_{\text{HOH}^+ - \text{HO}}^0)$. This criteria can be used to discriminate between compounds behaving as doubly charged or as two monocharged ions with respect to partition, but the boundary between these two limiting cases is difficult to establish, because of the difficulty of finding a physical model linking the intramolecular separation of the charges to the partition coefficient of a compound.

These results show that the good separation between the charges borne by an ion as well as the possibility of delocalising these charges over a large distance greatly favours the transfer of a compound into the organic phase. This enhancement of ion lipophilicity could affect drug–membrane interactions, and thus the regulation of drug transport. Since the amount of available data on partition coefficients of ionisable drugs (work is in progress in our laboratories) is increasing, it should soon be possible to include charge distributions in quantitative structure–activity relationship studies.

Conclusions

The approach described in this paper leads to an improved understanding of charge transfer reactions at the ITIES and of the physicochemical molecular mechanisms of passive transfer of organic ions. The electrochemical technique allows the precise determination of the distribution of ionic species between two phases, and ionic partition diagrams can be used as a first approach in the examination of the implications of ion partitioning in drug transport and delivery.

Born's ion–solvent interaction model also suggests that, when they transfer into the organic phase, compounds with a completely localised charge are solvated in a similar manner to that of small ions, whereas compounds possessing a well-delocalised charge behave like larger ions, because the smaller the molecular radius the more negative the corresponding $\text{diff}(\log P_{\text{T-N}}^0)$ value. Born's model also tends to show that the intramolecular distance between the charges plays a very important role with multiply charged ions. Indeed, the results obtained with quinine indicate that, with respect to solvation, its doubly charged form behaves as two monocations rather than as a dication, because its $\text{diff}(\log P_{\text{T-N}}^0)$ value is only twice that of $\text{diff}(\log P_{\text{T-N}}^0)$.

The difference between the partition coefficients of the neutral and ionised forms of a solute affords valuable information about the effect of the charge on the lipophilicity. This is a rather novel physicochemical parameter and it has been shown to encode intramolecular factors of a geometric and electronic nature (such as intramolecular distances, delocalisation and resonance), which is indicative of the solvation properties of ions in different media and of partial charge neutralisation.

The present study also shows qualitatively that the partitioning of ionic species can be related not only to the charge distribution around the molecule (electrostatic field) but also, and perhaps mainly, to the delocalisation (stabilisation) of the charge inside the molecule. To be able to quantify the main

forces (electrostatic and/or hydrophobic association^[15, 41, 42]) which influence the partitioning of ionic species, careful investigation of their electronic structure should be carried out. Standard techniques of computational chemistry, such as molecular mechanics, molecular dynamics, semiempirical and ab initio quantum calculations could be applied for the exploration of the conformational hypersurface of ionic species^[43–47] and for the study of their electronic structure and molecular electrostatic potentials.^[48–50] Such insights into quantitative structure–property relationships^[51] should allow a long-sought understanding of the real contribution of ionised forms to the distribution of drugs in the body.

Acknowledgements

P.-A.C., H.H.G. and B.T. are grateful for financial support by the Swiss National Science Foundation. Laboratoire d'Electrochimie is part of the European Training and Mobility Network on Organisation, Dynamics and Reactivity at Electrified Liquid/Liquid Interfaces (ODRELLI).

- [1] M. Karelson, V. S. Lobanov, A. R. Katritzky, *Chem. Rev.* **1996**, *96*, 1027–1043.
- [2] C. J. Cramer, D. G. Truhlar, Continuum Solvation Models: Classical and Quantum Mechanical Implementations in *Reviews in Computational Chemistry*, Vol. 6 (Eds.: K. B. Lipkowitz, D. B. Boyd), VCH, New York, **1995**, pp. 1–72.
- [3] C. Reichardt, *Solvents and Solvent Effects in Organic Chemistry*, 2nd ed., VCH, New York, **1990**.
- [4] E. Nakashima, R. Matsushita, T. Ohshima, A. Tsuji, F. Ichimura, *Drug Metabol. Dispos.* **1995**, *23*, 1220–1224.
- [5] V. Hiep Le, B. C. Lippold, *Int. J. Pharm.* **1995**, *124*, 285–292.
- [6] A. C. Chakrabarti, I. Clark-Lewis, P. R. Cullis, *Biochemistry* **1994**, *33*, 8479–8485.
- [7] G. M. Pauledti, H. Wunderli-Allenspach, *Eur. J. Pharm. Sci.* **1994**, *1*, 273–282.
- [8] E. de Paula, S. Schreier, *Biochim. Biophys. Acta* **1995**, *1240*, 25–33.
- [9] D. A. Smith, B. C. Jones, D. K. Walker, *Med. Res. Rev.* **1996**, *16*, 243–266.
- [10] A. Pagliara, P.-A. Carrupt, G. Caron, P. Gaillard, B. Testa, *Chem. Rev.* **1997**, *97*, 3385–3400.
- [11] R. P. Austin, A. M. Davis, C. N. Manners, *J. Pharm. Sci.* **1995**, *84*, 1180–1183.
- [12] H. H. Girault, Charge Transfer across Liquid/Liquid Interfaces in *Modern Aspects of Electrochemistry*, Vol. 25 (Eds.: J. O. M. Bockris, B. Conway, R. White), Plenum, New York, **1993**, pp. 1–62.
- [13] F. Reymond, G. Steyaert, P.-A. Carrupt, B. Testa, H. H. Girault, *Helv. Chim. Acta* **1996**, *79*, 101–117.
- [14] B. A. Moyer, Y. Sun, Principles of Solvent Extraction of Alkali Metal Ions: Understanding Factors Leading to Cesium Selectivity in Extraction by Solvation in *Ion Exchange and Solvent Extraction*, Vol. 13 (Eds.: J. A. Marinsky, Y. Marcus), Marcel Dekker, New York, **1997**, pp. 295–391.
- [15] M. H. Abraham, J. Liszi, *J. Inorg. Nucl. Chem.* **1981**, *43*, 143–151.
- [16] International program on chemical safety, 1,2-Dichloroethane in *Environmental Health Criteria*, Vol. 176, 2nd ed., World Health Organization, Geneva, **1995**.
- [17] T. Wandlowski, V. Marecek, Z. Samec, *Electrochim. Acta* **1990**, *35*, 1173–1175.
- [18] Y. Shao, S. G. Weber, *J. Phys. Chem.* **1996**, *100*, 14714–14720.
- [19] Y. Shao, A. A. Stewart, H. H. Girault, *J. Chem. Soc. Farad. Trans.* **1991**, *87*, 2593–2597.
- [20] F. Reymond, G. Steyaert, P.-A. Carrupt, B. Testa, H. H. Girault, *J. Am. Chem. Soc.* **1996**, *118*, 11951–11957.
- [21] A. Sabela, V. Marecek, Z. Samec, R. Fuoco, *Electrochimica Acta* **1992**, *37*, 231–235.

- [22] D. Perregaux, C. A. Gabel, *J. Biol. Chem.* **1994**, *269*, 15195–15203.
- [23] G. Caron, A. Pagliara, P. Gaillard, P.-A. Carrupt, B. Testa, *Helv. Chim. Acta* **1997**, *79*, 1683–1695.
- [24] F. Reymond, G. Steyaert, A. Pagliara, P.-A. Carrupt, B. Testa, H. Girault, *Helv. Chim. Acta* **1996**, *79*, 1651–1669.
- [25] R. I. Fox, H. I. Hang, *Lupus* **1993**, *2*, S9–S12.
- [26] R. Laliberte, D. Perregaux, L. Svensson, C. J. Pazoles, C. A. Gabel, *Cytokine* **1994**, *7*, 196–208.
- [27] P. McNiff, R. P. Robinson, C. A. Gabel, *Biochemical Pharmacology* **1995**, *50*, 1421–1432.
- [28] G. Steyaert, G. Lisa, P.-A. Carrupt, B. Testa, F. Reymond, H. H. Girault, *J. Chem. Soc. Faraday Trans.* **1997**, *93*, 401–406.
- [29] B. D'Epenoux, P. Seta, Amblard G., C. Gavach, *J. Electroanal. Chem.* **1979**, *99*, 77–84.
- [30] F. Reymond, G. Steyaert, P.-A. Carrupt, D. Morin, J.-P. Tillement, H. H. Girault, B. Testa, *The pH-Partition Profile of the Anti-Ischemic Drug Trimetazidine May Explain Its Reduction of Intracellular Acidosis*, submitted.
- [31] N. J. White, *Br. J. Clin. Pharmacol.* **1992**, *34*, 1–10.
- [32] D. J. Krogstad, P. H. Schlesinger, I. Y. Gluzman, *J. Cell. Biol.* **1985**, *101*, 2302–2309.
- [33] D. J. Krogstad, P. H. Schlesinger, *New Engl. J. Med.* **1987**, *317*, 542–549.
- [34] D. J. Krogstad, P. H. Schlesinger, *Biochem. Pharmacol.* **1986**, *35*, 547–552.
- [35] H. Ginsburg, E. Nissani, M. Krugliak, *Biochem. Pharmacol.* **1989**, *38*, 2645–2654.
- [36] *The Pharmacological Basis of Therapeutics* (Eds.: J. G. Hardman, L. E. Limbird, P. B. Molinoff, R. W. Ruddon, A. Goodman Gilman), 9th ed., McGraw-Hill, New York, **1995**.
- [37] D. L. Vander Jagt, L. A. Hunsaker, N. N. Campos, *Molec. Biochem. Parasitol.* **1986**, *18*, 389–400.
- [38] T. Yasuhara, M. Mori, K. Walamatsu, K. Kubo, *Biochem. Biophys. Res. Commun.* **1991**, *178*, 95–103.
- [39] A. F. G. Slater, A. Cerami, *Nature* **1992**, *355*, 167–169.
- [40] R. F. Rekker, R. Mannhold, *Calculation of Drug Lipophilicity. The Hydrophobic Fragmental Approach*, VCH, Weinheim, **1992**.
- [41] E. Tomlinson, S. S. Davis, *J. Colloid & Interface Sci.* **1980**, *76*, 563–572.
- [42] W. Kunz, P. Calmettes, T. Cartailier, P. Turq, *J. Chem. Phys.* **1993**, *99*, 2074–2077.
- [43] B. Walther, P.-A. Carrupt, N. El Tayar, B. Testa, *Helv. Chim. Acta* **1989**, *72*, 507–517.
- [44] C. Altomare, P.-A. Carrupt, N. El Tayar, B. Testa, T. Nagatsu, *Helv. Chim. Acta*, **1991**, *74*, 290–296.
- [45] P.-A. Carrupt, B. Testa, A. Bechalany, N. El Tayar, P. Descas, D. Perrissoud, *J. Med. Chem.* **1991**, *34*, 1272–1275.
- [46] H. H. Tennesen, J. V. Greenhill, *Int. J. Pharm.* **1992**, *87*, 79–87.
- [47] C. Altomare, S. Cellamare, A. Carotti, G. Casini, M. Ferappi, E. Gavuzzo, F. Mazza, P.-A. Carrupt, P. Gaillard, B. Testa, *J. Med. Chem.* **1995**, *38*, 170–179.
- [48] P.-A. Carrupt, N. El Tayar, A. Karlen, B. Testa, *Molecular Electrostatic Potential for Characterising Drug-Biosystem Interactions in Methods in Enzymology, Vol. 203*, Academic Press, London, **1991**, pp. 638–677.
- [49] E. D. Getzoff, D. E. Cabelli, C. L. Fisher, H. E. Parge, M. S. Viezzoli, L. Banci, R. A. Hallewell, *Nature* **1992**, *358*, 347–351.
- [50] M. K. Gilson, M. E. Davis, B. A. Luty, J. A. McCammon, *J. Phys. Chem.* **1993**, *97*, 3591–3600.
- [51] H. van de Waterbeemd, R. Mannhold, *Lipophilicity Descriptors for Structure–Property Correlation Studies: Overview of Experimental and Theoretical Methods and a Benchmark of logP Calculations in Lipophilicity in Drug Action and Toxicology, Vol. 4* (Eds.: V. Pliska, B. Testa, H. van de Waterbeemd), VCH, Weinheim, **1996**, pp. 401–418.
- [52] F. Reymond, V. Chopineaux-Courtois, G. Steyaert, G. Bouchard, P.-A. Carrupt, B. Testa, H. M. Girault, *Tonic Partition Diagrams of Ionizable Drugs: pH-Lipophilicity Profiles Transfer, Mechanisms and Charge Effects on Solvation, J. Electroanal. Chem.* in press.

Received: May 18, 1998 [F1160]